CCN production by new particle formation in the free troposphere

C. Rose[1], K. Sellegri[1], I. Moreno[2], F. Velarde[2], M. Ramonet[3], K. Weinhold[4], R. Krejci[5], M. Andrade[2], A. Wiedensohler[4], P. Ginot[6] and P. Laj[7]

[1] Laboratoire de Météorologie Physique CNRS UMR 6016, Observatoire de Physique du Globe de Clermont-Ferrand, Université Blaise Pascal, 24 avenue des Landais, 63171 Aubière, France

[2] Universidad Mayor de San Andres, LFA-IIF-UMSA, Laboratory for Atmospheric Physics, Campus Universitario Cota Cota calle 27, Edificio FCPN piso 3, Casilla 4680, La Paz, Bolivia

[3] Laboratoire des Sciences du Climat et de l'Environnement, LSCE/IPSL, CEA-CNRS-UVSQ, Université Paris-Saclay, F-91191, Gif-sur-Yvette, France

[4] Leibniz Institute for Tropospheric Research, Permoserstr. 15, 04318 Leipzig, Germany

[5] Department Environmental Science and Analytical Chemistry (ACES), Atmospheric Science Unit, Stockholm University, S 10691 Stockholm, Sweden

[6] Université Grenoble Alpes, CNRS, IRD, OSUG, F-38000 Grenoble, France

[7] Université. Grenoble Alpes, CNRS, IRD, IGE, F-38000 Grenoble, France

Abstract

Global models predict that new particle formation (NPF) is, in some environments, responsible for a substantial fraction of the total atmospheric particle number concentration and subsequently contribute significantly to cloud condensation nuclei (CCN) concentrations. NPF events were frequently observed at the highest atmospheric observatory in the world, Chacaltaya (5240 m a.s.l.), Bolivia. The present study focuses on the impact of NPF on CCN population. Neutral cluster and Air Ion Spectrometer and mobility particle size spectrometer measurements were simultaneously used to follow the growth of particles from cluster sizes down to ~2 nm up to CCN threshold sizes set to 50, 80 and 100 nm. Using measurements performed between January 1 and December 31 2012, we found that 61% of the 94 analysed events showed a clear particle growth and significant enhancement of the CCN-relevant particle number concentration. We evaluated the contribution of NPF relative to the transport and growth of pre-existing particles to the CCN-size. The averaged production of 50 nm particles during those events was 5072 cm^{-3}, and 1481 cm^{-3} for 100 nm particles, with a larger contribution of NPF compared to transport, especially during the wet season. The data set was further segregated into boundary layer (BL) and free troposphere (FT) conditions at the site. The NPF frequency of occurrence was higher in the BL (48%) compared to the FT (39%). Particle condensational growth was more frequently observed for events initiated in the FT, but on average faster for those initiated in the BL, when the amount of condensable species was most probably larger. As a result, the potential to form new CCN was higher for events initiated in the BL (67% against 53% in the FT). In contrast, higher CCN number concentration increases were found when the NPF process initially occurred in the FT, under less polluted conditions. This work highlights the competition between particle growth and the removal of freshly nucleated particles by coagulation processes. The results support model predictions which suggest that NPF is an effective source of CCN in some environments, and thus may influence regional climate through cloud related radiative processes.

1 Introduction

Atmospheric aerosol particles are known to affect air quality, health (Seaton et al., 1995) and climate. Beside their direct interaction with the solar and telluric radiations, aerosol particles also act as condensation nuclei for cloud droplets. Cloud effects such as cloud albedo (Twomey, 1977) and lifetime (Albrecht, 1989) constitute the largest uncertainty in the estimation of the radiative forcing of the Earth's atmosphere (IPCC, 2013).

The interaction between aerosol particles and the formation of warm clouds relies on the ability of the particles to serve as cloud condensation nuclei (CCN), which depends on the water vapour supersaturation, particle size distribution and also the chemical composition (e.g.: Roberts et al., 2010; Wex et al., 2010; Asmi et al., 2012). Besides the processing of primary particles, other CCN sources were identified, such as regional new particle formation (NPF) events (Kerminen et al., 2012).

NPF is a frequent atmospheric phenomenon including the formation of nanometer-sized clusters from gaseous precursors and their subsequent growth to larger sizes (eg. Kulmala and Kerminen, 2008). Typical growth rates between 1.8 and 10.7 nm h^{-1} were found for particles in the range 1.5 – 20 nm (Yli-Juuti et al., 2011), meaning that a few hours to a few days are needed for nucleated particles to grow to CCN sizes, around 50-150 nm (Kerminen et al., 2012). The chance for these clusters to grow to CCN sizes strongly depends on the competition between condensational growth and their removal by coagulation onto pre-existing particles.

During the last few years, several global model investigations were dedicated to the study of the CCN-size aerosol production attributed to atmospheric NPF (Makkonen et al., 2012; Merikanto et al., 2009; Reddington et al., 2011; Spracklen et al., 2008). While the outcomes of these different models may vary according to the way they treat NPF and aerosol particle processes (Lee et al., 2013), most of them show an enhancement of the CCN number concentration due to NPF, both in the boundary layer (BL) and in the free troposphere (FT). Based on the study by Makkonen et al. (2012), predictions of the present day annual global average CCN concentration in the BL show almost a fivefold increase when taking into account NPF. According to Merikanto et al. (2009), 45% of global low-level cloud CCN at 0.2% supersaturation originate from nucleation, and 35% have been formed in the free and upper troposphere. Slightly contrasting results are provided by Reddington et al. (2011) using the global model GLOMAP against measurements conducted at 15 European ground based stations in the frame of the EUCAARI project. Reddington and co-workers found that CCN-sized particle concentrations in the BL were mainly driven by processes other than NPF, which contributed significantly to the CCN budget at little less than a quarter of observational sites included in the study.

However, observations to validate these predictions are scarce, especially for the FT, where measurements are often technically challenging. Recent studies conducted at the Jungfraujoch station (Switzerland, 3580 m a.s.l.) reported significant enhancement of the particle concentration below 50 nm by NPF in the FT, while only a minor fraction of this particles grow beyond 90 nm, even on a time scale of several days (Herrmann et al., 2015; Tröstl et al., 2016). The contribution of NPF to the production of CCN is thus likely to be very limited in this part of the FT, while boundary layer originating particles were observed to dominate the CCN concentrations measured at Jungfraujoch. The occurrence of the NPF process itself in the FT was reported to be tightly connected with the strength of boundary layer influence at the site, together with global radiation (Bianchi et al., 2016; Tröstl et al., 2016).

In this context, the purpose of the present study is to estimate the contribution of NPF to CCN formation at the station of Chacaltaya (5240 m a.s.l., Bolivia) with a special attention in differentiating the CCN number concentrations attributed to NPF and particle growth occurring at the station from those attributed to the transport of pre-existing CCN-size particles to the site. This analysis was performed using an indirect method based on the NPF event classification previously reported by Rose et al., (2015a) and particle number size distribution measurements in the range 10-500 nm. In addition to global CCN number concentrations, a more detailed analysis of NPF and subsequent CCN production in the BL or in the FT is also reported.

2 Measurements and methods

2.1 Observation site and instruments

Aerosol particle number size distributions, together with routine meteorological parameters, were measured at the Chacaltaya GAW station, located in a range of the Bolivian Andes at the summit of Mount Chacaltaya (16°21.014' S, 68°07.886' W), 15 km North of La Paz – El Alto metropolitan area (2 million inhabitants).

The mobility distribution of charged particles and ions (3.2 – 0.0013 $cm^2V^{-1}s^{-1}$) and the size distribution of total particles (2 – 42 nm) were measured by a Neutral cluster and Air Ion Spectrometer (NAIS, Airel Ltd., Mirme and Mirme, 2013). The NAIS sampled the ambient aerosol through an individual non-heated short inlet (~ 50 cm) with a 5 minute time resolution. Since the NAIS was likely to overestimate particle number concentrations above 20 nm (Manninen et al., 2016), particles in the range from 20 nm to CCN relevant sizes were preferentially measured using a mobility particle size spectrometer type TROPOS-SMPS (Wiedensohler et al., 2012). The SMPS operated behind a Whole Air Inlet equipped with an automatic dryer.

More details on the measurement site as well as the instrumental setup and the data quality assurance can be found in Rose et al. (2015a) and Andrade et al. (2015).

2.2 Method to assess the local influence of the boundary layer in Chacaltaya

In order to assess whether the site is under the influence of the planetary boundary layer or the low free troposphere at a local scale, regardless the history of the air mass, we employed the hourly-averaged value of the standard deviation of the horizontal wind direction (σ_θ).

The value of σ_θ has been extensively used in air pollution monitoring (EPA, 2008; Mitchell, 1982; Mitchell and Timbre, 1979; Weber, 1997) and dispersion models as an indicator of the stability of the lower atmosphere. Instable atmospheric conditions produce turbulence and therefore high wind variability. Conversely, low wind variability due to stable conditions produces low σ_θ values. In Chacaltaya, σ_θ was used from a mountain perspective, .i.e.

assuming that turbulent conditions ($\sigma_\theta \geq 12.5$) reflect the influence of the BL at the observatory and, contrarily, that non-turbulent (or stable) conditions are equivalent of being in the FT (σ_θ <12.5).

In Chacaltaya, σ_θ is obtained at the summit (5380 m a.s.l., 10 m above the surface) by means of a wind vane and propeller (Young 05103) and processed directly on a CS-CR1000 datalogger. σ_θ is defined as the standard deviation of the horizontal wind direction itself according to Eq. (1), but its value is approximated by the Yamartino (1984) single-pass method (set of Eq. (2)) directly in the datalogger.

$$\sigma_\theta = \left[\frac{\sum_{i=1}^{N} (\theta_i - \theta_A)^2}{N-1} \right]^{\frac{1}{2}} \tag{1}$$

where θ_i is the instantaneous wind direction and θ_A the average wind direction.

$$\begin{aligned} \sigma_\theta &= \arcsin(\varepsilon)\left[1 + \left(\frac{2}{\sqrt{3}} - 1\right)\varepsilon^3\right] \\ \varepsilon &\equiv \sqrt{1 - (S^2 + C^2)} \\ S &= \frac{1}{N}\sum_{i=1}^{N} \sin\theta_i \\ C &= \frac{1}{N}\sum_{i=1}^{N} \cos\theta_i \end{aligned} \tag{2}$$

The synoptically driven change of wind direction may affect the calculation of σ_θ for short time periods. This low-frequency horizontal wind oscillation is called “meandering” and may produce overestimation of σ_θ during situations of low wind speed (≤ 2m.s^{-1}), which usually take place during daytime in Chacaltya. Therefore, 15-min averaged values are calculated offline according to Eq. (3) to avoid wind meandering effects.

$${\sigma_{\theta(1-hr)}}^2 = \frac{\sigma^2_{\theta(15)} + \sigma^2_{\theta(30)} + \sigma^2_{\theta(45)} + \sigma^2_{\theta(60)}}{4} \tag{3}$$

where every $\sigma_{\theta(15x)}$ equation is a 15-minute deviation of the wind direction.

The threshold set for stable FT conditions is $\sigma_\theta \geq 12.5$, following Mitchell’s recommendations (1982). In Chacaltaya, FT conditions take place usually during night-time and before sunrise, as it would be expected for mountain sites. Nevertheless, in many cases σ_θ values lower than

18 are observed in a persistent pattern (more than 4 hours of this condition). This may indicate the existence of a residual or interface layer (IL). This intermediate layer would not correspond neither to the FT nor the proper BL. Moreover, during the wet season, convective and unstable conditions produce more turbulence at the site, shifting the σ_θ towards higher values, typically below 18. Therefore other secondary site specific thresholds are applied, namely 18 and 22.5.

Obtained hourly dataset is then checked for consistency, in particular with black carbon measurements, and the following smoothing is applied. We establish a 4-hour window (2h before and 2h after the data point of interest) into which the following criteria are applied:

- If the σ_θ value is lower than 12.5 (classified as FT), but if it is the only data point in the 4-hour window, it is not considered as FT and it is reclassified as an IL point instead.
- If the σ_θ value is lower than 18 and 75% of the points in the 4-hour window are lower than 12.5, the point is classified as a FT point (stable).
- If the σ_θ value is lower than 22.5 and 75% of the points in the 4-hour window are lower than 18, the point is classified as an IL point (this takes place mostly during the wet season).

3 Results

3.1 CCN formation during and from NPF

3.1.1 Investigation of total CCN formation during NPF events

In absence of direct CCN measurements at Chacaltaya, the contribution of NPF to CCN production was estimated from the continuous monitoring of the particle number size distribution. This indirect method was first introduced by Lihavainen et al. (2003) and has already been used in several other studies (Asmi et al., 2011; Kerminen et al., 2012; Laakso et al., 2013; Laaksonen et al., 2005).

The basic hypothesis is that the lower cloud droplet activation diameter of aerosol particles is in the range 50-150 nm for the usual supersaturations encountered in natural clouds (Asmi et al., 2011, 2012; Komppula et al., 2005) including those forming at altitudes up to 3580 m a.s.l., as observed at the Jungfraujoch station (Switzerland) (Hammer et al., 2014; Jurányi et al., 2011). Although these conditions might be slightly different from those found in clouds forming above 5000 m, we assume that on a first approach the CCN sizes previously mentioned apply the same way at such altitudes. Thus, CCN number concentrations are assimilated to a range of three different CN concentrations: hereafter, CCN_{50} and CCN_{100} refer to the higher and lower limits of the CCN concentration estimated from the number concentrations of particles larger than 50 nm and 100 nm, respectively; as additional information, an intermediate CCN concentration (CCN_{80}) was deduced from the number concentration of particles larger than 80 nm. The CCN production during an event was obtained from the comparison of the CCN concentration N_{init} prior to and the maximum CCN concentration N_{max} during the event. For each particle diameter range, N_{init} is defined as the 30 minute average concentration obtained at t_{init}, when growing particles reach the threshold size, whereas N_{max} is the 30 minute average concentration calculated when the CCN concentration reaches a maximum during an event, at t_{max}. The determination of N_{init} and N_{max} is depicted on Fig. 1. It is worth noticing that this indirect method based on particle size only provides estimations of potential CCN concentrations instead of real concentrations as measured by CCN chambers (Roberts and Nenes, 2005). However, for simplicity, we refer to these potential CCN as CCN hereafter.

The selection of the NPF events to be analyzed was performed based on the following criteria First, only those NPF events referred as type I, i.e. with clear particle growth from smallest sizes, were considered; they contrast with type II events, during which the growth is more irregular and may be interrupted in certain size ranges, and bump type events, which completely miss the growth of the newly formed clusters (Hirsikko et al., 2007; Yli-Juuti et al., 2009). Second, the days showing an eventual contribution from NPF events triggered the day before were rejected. Especially, those days when the NPF contribution superimpose on that from a strong growing pre-existing Aitken mode band (of similar or even larger intensity in terms of particle concentration), as previously described by Tröstl et al. (2016), were removed from the analysis. Regarding this aspect, our analysis is thus a lower limit of the contribution of NPF to CCN-size relevant aerosol concentrations.

During the measurement period January 1 to December 31 2012, 147 days showing type I NPF events were detected: 112 during the dry season, from May to October, and 35 during the wet season, from November to April (Rose et al., 2015a). However, because of missing data of particle number size distribution measurements, only 94 of them were further analysed (75 from the dry season and 19 from the wet season).

Over the whole year, 61% of the studied NPF events were apparently growing to CCN-relevant sizes, and when observed, the contribution of growing particles to CCN concentrations was systematically seen up to at least 100 nm. During the wet season, the frequency of aerosol particles reaching CCN sizes during a NPF event was higher compared to the dry season (79 % and 56%, respectively). This last observation can be ascribed to the larger growth rates which were detected during the wet season, being on average enhanced by a factor 1.7 compared to the dry season (Rose et al., 2015a). It is however worth noticing that at this stage, the contribution of pre-existing particles transported to the site at already grown sizes cannot be excluded.

Our results of CCN concentration increase during NPF events can be compared to literature values obtained using similar methodologies for other sites. The results reported by Asmi et al. (2011) for Pallas (560 m a.s.l., Finland) slightly contrast with these observations. Indeed, the CCN number concentration increase during NPF events showed a seasonal variation but also decreased with increasing activation diameter. This might be explained by a decreasing availability of condensing vapours over the course of the particle growth time period. At Chacaltaya, the availability of condensing gases appears to increase over a large time period, sometimes reaching concentrations that trigger a second (and third) nucleation event during the same day, in spite of the raising condensable sink due to the first nucleation event (Rose et al., 2015a). Coagulation processes however lead to a decrease of CCN_{100} compared to CCN_{50}. This is illustrated on Figure 2.a, which shows, for the three threshold sizes and for each season, the median CCN concentration increase observed during NPF events and calculated as the difference between N_{max} and N_{init}. Considering all type I event days over the whole year, the median number concentration of new CCN produced during a NPF event was 5072 cm^{-3} for CCN_{50}, 2254 and 1481 cm^{-3} for CCN_{80} and CCN_{100}, respectively. The number concentration of new CCN was on average higher during the dry season, especially for CCN_{50}.

Corresponding relative increases in CCN number concentration were calculated as the ratio of the absolute increases previously reported over N_{init}, i.e. the 30 min average CCN number concentration measured when growing particles initially reach the threshold sizes (Fig. 2.b). CCN concentrations were found to increase by 168 to 996% at Chacaltaya during NPF events, with no clear differences between seasons or threshold sizes.

One should note that when several consecutive type I events were detected on a same day (this occurred on 7 occasions), it was complex to extract the contribution of each individual event, so the calculated CCN production was the result of the contribution of all events as a whole. During multiple events days, the median number concentration of CCN produced was on average 1.7 times higher compared to single type I event days.

As previously mentioned, similar methodologies were used in previous studies to evaluate the increase of CCN concentrations during NPF events. The average absolute CCN production observed during NPF events at Chacaltaya is lower compared to that reported by Laaksonen et al., (2005) at the station of San Pietro Capofiume located in the polluted region of the Pô valley (11 m a.s.l., Italy): on the basis of 304 NPF events, the average number of new CCN produced during an event are 7.3×10^3 cm^{-3} and 2.4×10^3 cm^{-3}, for CCN_{50} and CCN_{100}, respectively. In contrast, the values from both Chacaltaya and San Pietro Capofiume are significantly higher than those reported by Kerminen et al. (2012) for the stations of Botsalano (1420 m a.s.l., South Africa), Vavihill (172 m a.s.l., Sweden), Pallas and Hyytiälä (182 m a.s.l., Finland). Among these four sites, the highest CCN concentration increases are on average observed at Botsalano (2500 cm^{-3}, 1400 $cm^{-3}$and 800 cm^{-3} for CCN_{50}, CCN_{80} and CCN_{100}, respectively), whereas Pallas displays the lowest CCN production (1000 cm^{-3}, 250 $cm^{-3}$and 150 cm^{-3} for CCN_{50}, CCN_{80} and CCN_{100}, respectively). Corresponding relative increases in CCN concentrations found in the literature are always larger than 100% but never exceed 400%, being thus on average significantly lower than those observed at Chacaltaya. However, it is worth noticing that these contrasting results may arise from the various conditions that are found at the different stations, especially regarding altitude and pollution levels, thus influencing NPF both in terms of strength, spatial extend and temporal evolution.

The potential of NPF to contribute to CCN production at high altitude was more particularly investigated by Tröstl et al. (2016) at the Jungfraujoch station. Tröstl and co-workers found that newly formed particles did not directly grow to CCN sizes (90 nm at Jungfraujoch) within observable time scale (up to two days) but rather experienced a multi-step growth process over several days. As a consequence, the contribution of NPF to the CCN budget was complex to distinguish from that of other sources such as BL entrainment of larger particles, which was likely the main source of measured CCN. At Mount Whistler (2182 m a.s.l., Canada), Pierce et al. (2012) followed a different approach including calculations of the probability for freshly nucleated particles to reach CCN relevant sizes. Based on a five event day period, they found that in absence of high coagulation/condensation sinks, up to 24% of the newly formed clusters could grow to at least 100 nm, thus forming potential CCN.

As previously mentioned, the vertical transport of aerosol particles from lower atmospheric levels that takes place after sunrise concurrently to NPF may represent a significant contribution to the increase of CCN-relevant size particle number concentrations at these mountain sites. This aspect will be addressed in the next section, in which the contribution of NPF is further compared with the CCN number concentration increase resulting from the transport of particles to the site.

The seasonal and annual CCN productions related to NPF events were estimated from 1) the average fraction of type I NPF events contributing to the formation of new CCN reported above, 2) the frequency of occurrence of type I NPF events at the site and 3) the average CCN number concentration increase measured for those type I events during which growing particles reached the potential CCN activation diameter. As an example, the CCN_{50} production during the wet season was calculated as follows:

$$CCN_{50-wet} = frac_{wet} \times tot\_nb_{wet} \times avg\_conc_{wet} = 79\% \times 35 \times 3070 = 8.48 \times 10^{4}\, cm^{-3} \quad (4)$$

where, for each season, $frac$ is the fraction of NPF events leading to CCN concentration increase, tot_nb is the total number of days showing type I events and avg_conc is the median number of new CCN formed during an event. Similar calculations were done for each season and CCN class, leading to the values reported in Table 1. The annual CCN production was calculated as the sum of the seasonal productions.

Based on Table 1, the CCN production at Chacaltaya was higher during the dry season compared to the wet season for all CCN classes, but especially for CCN_{50}, which was more than 4 times higher compared to the wet season. The annual CCN production calculated at San Pietro Capofiume is 3.4×10^{5} cm^{-3} and 1.1×10^{5} cm^{-3}, for CCN_{50} and CCN_{100}, respectively (Laaksonen et al., 2005). These values are slightly lower than those obtained at Chacaltaya, despite the fact that the median number of potential new CCN formed during an event is on average higher in San Pietro Capofiume. This last observation can be ascribed to the high NPF frequency at Chacaltaya, together with the significant fraction of type I events and high growth rates (Rose et al., 2015a).

3.1.2 Estimation of CCN formation from NPF alone

The aim of this section is to evaluate the contribution of particles transported to the site to the total CCN concentration and give an estimation of the CCN production from NPF alone.

In fact, in addition to the previous analysis classically used in the literature, further calculations are needed to take into consideration the geographical specificity of the site. Indeed, if NPF contributes to the formation of potential new CCN, pre-existing particles in the CCN size range transported to the site by diurnal forced or heat convection might also, in parallel, lead to an apparent increase of the CCN number concentration. Thus, the CCN number concentrations estimated using the methodology previously described, and attributed to NPF in a first approach, might in fact result from both NPF and transport. The transport of particles to the site is taken into account based on the hypothesis that similar number concentrations of particles are transported to the site on event and non-event days. The contribution of NPF to the production of new CCN was thus estimated from the difference between the median CCN increases obtained on event (contributions from NPF and transport) and non-event days (transport only).

Among the 362 days included in this analysis, 108 (23 and 85 during the dry and wet season respectively) were identified as non-event days, but only 78 of them (22 from the dry season and 56 from the wet season) were further analysed because of instrumental failures. The median diurnal variation of CCN_{50} obtained on these non-event days and attributed to transport is shown on Fig. 3, together with the median number concentrations obtained on event days and ascribed to both NPF and transport (upper panel). Similar figures are reported in the supplementary material for CCN_{80} and CCN_{100} (Figures S1 and S2, respectively). As previously mentioned, the contribution of NPF to the production of new CCN was estimated from the difference between the median CCN_{50} increases obtained on event and non-event days and is shown on Fig. 3 (lower panel). This absolute CCN production from NPF alone is also reported, together with the corresponding relative concentration increase, on Fig. 4 for further comparison with Fig. 2 (showing both transport and NPF contributions as a whole).

During the dry season, transport contributes to CCN_{80} and CCN_{100} to the median level of 1139 and 863 cm^{-3}, which is similar to the contribution of NPF (1229 and 784 cm^{-3} for CCN_{80} and CCN_{100}, respectively, Fig. S1, S2). In contrast, CCN_{50} attributed to NPF (3197 cm^{-3}) significantly exceeds the median number of particles transported to the site (1610 cm^{-3}) (Fig. 3). During the wet season, NPF is likely to be the dominant CCN source, with productions of

1950, 771 and 535 cm^{-3} for CCN_{50}, CCN_{80} and CCN_{100}, respectively, compared to median concentrations attributed to transport which do not exceed 690, 404 and 321 cm^{-3}. The contributions of NPF particles to the increase of CCN, all shown on Fig. 4.a. and reported in Table 2 for the different seasons and sizes, hence represent a significant fraction of the CCN increase shown on Fig. 2.a. and reported in Table 1. The contribution of NPF to CCN concentrations are comparable or even higher than those previously mentioned for other stations in the literature, which probably also include CCN sources other than NPF. The relative impact of NPF is estimated to increase the CCN_{50} number concentrations by more than 250 % during both seasons, and the CCN_{100} number concentrations by more than 100% and 200% during the dry season and wet season, respectively.

These calculations rely on the hypothesis that the specific environmental conditions on which NPF occurs are not influencing the transport from lower atmospheric layers. In order to further evaluate the reliability of this assumption, wind direction and speed as well as global radiation were investigated on event and non-event days (Figures S3 and S4 in the supplementary material). As previously reported by Rose et al. (2015a), NPF events are favoured during clear sky conditions, when radiation is higher (Fig. S3). Thus, there is likely a bias towards an underestimation of radiative driven transport from lower atmospheric layers due to the fact that cloudy days are over-represented for non-event days. Regarding wind, contrasting directions are also observed between event and non-event days (Fig. S4), with patterns closely related to those observed for the dry and wet seasons, respectively (Rose et al., 2015a). It is worth noticing that winds originating from the more polluted sector of La Paz – El Alto (south) do not seem to be over-represented neither on event nor on non-event days. However, because of the close proximity of this area, it is complex to further assess how it contributes to CCN concentration from wind direction alone, and we cannot exclude a bias related to the variability of this specific source between event and non-event days. Nonetheless, the particle number concentrations observed at the time preceding the usual occurrence of the NPF events are similar for event and non-event days (Fig 3, S1, S2). Moreover, higher wind speeds are on average recorded on non-event days, that likely lead to an enhanced transport of particles to the site compared to event days, and hence lead to an underestimation of the contribution of NPF to the increase of CCN. In any case, taking into account the contribution of transport when calculating the increase of CCN concentrations after NPF events was never done in the past, and certainly helps approaching a more realistic view of the real contribution of NPF to CCN number concentrations.

3.2 How layering influences growth to CCN-sizes

3.2.1 Occurrence of NPF in the different tropospheric layers

The purpose of this section is to further investigate NPF in terms of occurrence, event type and characteristics (particle formation and growth rate) regarding the location of the station in the tropospheric layers (i.e. BL, FT or IL) at the onset of the NPF process. The classification of air mass types into BL, IL and FT was obtained using the standard deviation of wind direction (Section 2.2).

389 NPF events (including all event types, i.e. I, II or bump) previously discussed by Rose et al. (2015a) were included in this analysis. For each event, the air mass type (BL, IL or FT) prevailing at the station was investigated on an hourly basis during the first steps of the NPF process, i.e. from the appearance of the newly formed clusters (< 3nm) to the time at which the concentration of 3-7 nm particles was maximum. There was no information available regarding the classification into BL, IL and FT for 56 events.

Various scenarios were observed during this part of the NPF process, which on average lasted for 2.7±1.3 hours. The most frequent scenarios, which include more than 88% of the documented events, are listed, together with their frequency of occurrence, in Table 3. Scenario S1 refers to those days when the first steps of the NPF process were observed to occur in the BL, while scenario S2 refer to the events started in the FT. Scenario S2 is further divided into two sub-classes to distinguish between the events which first steps occur exclusively in the FT (S2.1) from those during which BL dynamics lead to changing conditions in the course of the event (S2.2). Events triggered in the IL are not frequently observed compared to those initiated in the BL or in the FT, and are thus not highlighted in this classification. Since multiple events were frequently detected at Chacaltaya, additional information regarding the occurrence of the scenarios as a function of the event position (first event, second event, third and following events) is also provided. For that purpose, single events and events occurring first on multiple event days were considered all together, while second and following events were considered in a second category.

Based on Table 3, constant conditions, i.e. scenarios S1 (BL conditions only) and S2.1 (FT conditions only), were found in 64% of the selected single and first position events and 97%

of the second and following events. In each case, scenario S1, corresponding to BL conditions, was the most frequent, representing 93% and 96% of the events initiated in constant conditions, respectively for single and first position events and for second and following ones. The fact that scenario S2.2 related to changing conditions was more frequently observed for single and first position events (36% compared to 3% for following events), i.e. occurring earlier in the morning compared to following events, is mainly explained by the development of the BL during the first part of the day, as shown on Fig. 5.

NPF frequencies in the FT and in the BL were also deduced from the previous classification. For that purpose, the analysis was focused on the time period 08:00 - 12:00 (Local), which includes the most probable nucleation hours (Rose et al., 2015a). 72 days (including both event, non-event an undefined days) were rejected from the analysis because of missing information regarding the location of the station in the tropospheric layers. Free tropospheric conditions were detected during at least one hour on 122 days, and among these days, 48 showed NPF events initiated in the FT, leading to a NPF frequency of 39%. In contrast, the station laid in the BL during at least one hour on 248 days, and among these days, 119 showed events starting in the BL, leading to a NPF frequency of 48%.

3.2.2 Event type and characteristics

An additional analysis concerning the event type (i.e. I, II or bump) as a function of the scenario was performed using the event classification from Rose et al. (2015a). The results of this analysis are shown on Fig. 6. Almost half of the 77 events triggered in the FT (scenarios S2, Table 3) were identified as type I events (38 events), while types II and bump events were observed on 18 and 21 occasions, respectively, which represent 23 and 27% of scenario S2. When considering the scenarios S2.1 and S2.2 independently from one another, we found that type I events were predominant when changing conditions were detected (S2.2), whereas they displayed similar probabilities of occurrence as other event types in constant free tropospheric conditions (S2.1). This observation suggests that the probability for type I events to occur is increased when initial free tropospheric conditions are changing in the course of the events. This could be explained by favorable conditions for the onset of nucleation events, including sufficient amount of gaseous precursors and low coagulation sink preventing the loss of clusters, followed by increased input of condensable species from the BL promoting particle growth. However, this hypothesis must be considered with caution regarding the limited number of events occurring under scenario S2.1. Regarding scenario S1, in the BL, comparable number of events belonging to class I and II were reported (87 and 92 events, thus representing 40 and 42% of scenario S1, respectively).

In order to further characterize the NPF events in the different atmospheric layers, statistics regarding the formation rate of 2 nm particle and the growth rate (GR) in the size range 1-3 nm as a function of the scenarios were performed for type I events. Growth rates were derived from the particle number size distribution using the “maximum” method from Hirsikko et al. (2005), while formation rates were calculated according to Kulmala et al. (2007). Given the limited number of type I events observed in scenario S2.1 (4 events), scenarios S2.1 and S2.2 were not distinguished from each other in the statistics. As shown on Fig. 7, increased values are on average reported in the BL, with higher variability, especially for the GR. Additional analysis was performed to investigate the correlation between the GR in the size range 3-7 nm and the location of the station at the end of the scenarios. However, because of an insufficient number of values for events occurring under scenarios ending in the FT (scenario S2.1, 4 values), these results will not be further discussed.

We have shown so far that while higher NPF frequencies where found in the BL compared to the FT, higher probabilities for type I events to occur were associated to scenarios starting in the FT and ending in the BL or IL. However, when events belonging to class I are initiated in the BL, they show on average higher particle formation and growth rates compared to those started in the FT. Thus, it is likely that on the one hand higher amounts of gaseous precursors usually associated with the BL could favor nucleation events of higher intensity and explain both higher NPF frequencies and enhanced particle formation and growth rates. On the other hand, cleaner conditions found in the FT at the very beginning of the NPF process may reduce the sink for the newly formed clusters and favor their growth to larger sizes. This observation suggests that the amount of condensable species could directly influence the occurrence of the NPF process and determine the particle growth rate while the occurrence of the growth process itself could rather depend on the strength of the particle sink. Overall, the difference of occurrence frequency, nucleation rates and GR between FT and BL are not very large, and we show that nucleation is initiated in the FT with a rather high frequency.

The purpose of the next section is now to investigate the impact of these NPF events on the CCN number concentration in each of the atmospheric layers.

3.2.3 CCN production during NPF events in the different tropospheric layers

Based on the results discussed in section 3.1.1, 57 NPF event days showing particle growth up to CCN activation diameter were detected at Chacaltaya. 13 of them were not further analyzed due to missing information regarding the location of the station in the tropospheric layers. Among the remaining 44 days, 31 showed events initiated in the BL, 10 in the FT, 2 at the interface between the BL and the FT and 1 in random conditions. Given their limited number, events started in the IL will not be further discussed. The frequency of NPF contribution to the production of new CCN in the BL and in the FT was calculated as the ratio of NPF events growing to the CCN sizes to the total number of type I events occurring in each atmospheric layer, i.e. 46 in the BL and 19 in the FT. The resulting frequency of CCN production from NPF was 67% in the BL, being slightly higher compared to the FT (53%).

The number concentration of CCN formed during an event was also analyzed as a function of the air mass type (BL or FT) prevailing at the station (Table 4). Using the three threshold sizes, median CCN productions were comparable for events initiated in the BL and in the FT. In contrast, the third quartiles of CCN_{80} and CCN_{100} were higher for the events initiated in the FT.

The fact that the contribution of NPF to the formation of new CCN was more frequently observed for events initiated in the BL might be explained by faster particle growth sustained by higher amounts of condensable material, thus increasing the chances for particles to reach CCN sizes. The tendency for CCN_{80} and CCN_{100} to reach higher values when the NPF process was started in the FT can be due to smaller initial concentrations prior to the NPF event, and thus weaker coagulation associated to less polluted conditions in the FT.

Additional analysis regarding the history of the air mass and BL influence along its trajectory would provide valuable information to even more assess the role of the exchanges between the BL and the FT on the occurrence of NPF and its contribution to the formation of new CCN. Indeed, observations conducted at the Jungfraujoch showed that stronger NPF events (type I) occurred in air masses one or two days after contact with the BL (Bianchi et al., 2016; Tröstl et al., 2016). These results are however based on proxies (CO, NOy) and modelling tools which were unfortunately not available for Chacaltaya. Nevertheless, our results goes to some extent into the same direction as the work by Tröstl et al. (2016) and Bianchi et al. (2016), at least supporting the major role of BL intrusion (regardless of its kind, before or during the event) to sustain particle growth. Similar FT feeding process from the BL was also shown by Rose et al. (2015b) at the puy de Dôme (France, 1465 m a.s.l.).

4 Conclusion

In this paper, the contribution of NPF to the production of potential new CCN was investigated at the highest station in the world, Chacaltaya (5240 m a.s.l., Bolivia), between January 1 and December 31 2012.

Using potential CCN activation diameters 50, 80 and 100 nm, we found that 61% of the type I NPF events included in the analysis lead to CCN number concentration increase, with higher probabilities during the wet season (79%) explained by faster particle growth. Because of coagulation on pre-existing particles, the number concentration of CCN formed was observed to decrease with increasing activation diameter, but the frequency of particles reaching the highest potential CCN activation diameter (100nm) was not reduced compared to the lowest CCN size (50 nm). When comparing the CCN production from NPF with the number concentration of pre-existing CCN transported to the site, we found that NPF was on average responsible for the largest contribution to the CCN concentration, especially during the wet season.

When segregating into BL and FT air masses sampled at the site, we found slightly higher NPF frequency in the BL (48%) but still an important frequency of occurrence in the FT (nucleation frequency of 39%). This observation is, to our knowledge, the first of its kind. Particle growth was more frequently observed for events initiated in the FT but was on average faster for events started in the BL, most probably because of increased amounts of condensable vapours. As a result, the chance for particles to grow up to potential CCN activation diameters was higher when the NPF process occurred in the BL. In contrast, the impact of NPF initiated in the FT on CCN number concentrations was higher than for NPF initiated in the BL, most likely because of the decreased pollution levels and weaker coagulation sink. The previous observations clearly highlight the competition that exists between particle growth and their removal by coagulation processes on pre-existing particles, and thus the complex balance between sources and sinks that is required to observe the formation of new particles and their subsequent growth to climate relevant sizes. Such conditions are often fulfilled at Chacaltaya, where NPF seems to often play a dominant role in the formation of new CCN.

Acknowledgments

This work was performed within the framework of ACTRIS2 (Aerosols, Clouds and Trace gases Research InfraStructure) and received financial supports from IRD under JEAI CHARME project, CNRS-INSU under LEFE-CHAT and ACTRIS-FR programs, ANR under Labex OSUG@2020 (ANR10 LABX56) Investissement d'Avenir program as well as from STINT and FORMAS funding agencies.

References

Albrecht, B. A.: Aerosols, cloud microphysics, and fractional cloudiness, Science, 245(4923), 1227–1230, 1989.

Andrade, M., Zaratti, F., Forno, R., Gutiérrez, R., Moreno, I., Velarde, F., Ávila, F., Roca, M., Sánchez, M. F., Laj, P., Jaffrezo, J. L., Ginot, P., Sellegri, K., Ramonet, M., Laurent, O., Weinhold, K., Wiedensohler, A., Krejci, R., Bonasoni, P., Cristofanelli, P., Whiteman, D., Vimeux, F., Dommergue, A. and Magand, O.: Puesta en marcha de una nueva estación de monitoreo climático en los andes centrales de Bolivia: la estación Gaw/Chacaltaya, Revista Boliviana de Física, 26(26), 06-15, 2015.

Asmi, E., Kivekäs, N., Kerminen, V.-M., Komppula, M., Hyvärinen, A.-P., Hatakka, J., Viisanen, Y. and Lihavainen, H.: Secondary new particle formation in Northern Finland Pallas site between the years 2000 and 2010, Atmos. Chem. Phys., 11(24), 12959–12972, doi:10.5194/acp-11-12959-2011, 2011.

Asmi, E., Freney, E., Hervo, M., Picard, D., Rose, C., Colomb, A. and Sellegri, K.: Aerosol cloud activation in summer and winter at puy-de-Dôme high altitude site in France, Atmos. Chem. Phys., 12(23), 11589–11607, doi:10.5194/acp-12-11589-2012, 2012.

Bianchi, F., Tröstl, J., Junninen, H., Frege, C., Henne, S., Hoyle, C. R., Molteni, U., Herrmann, E., Adamov, A., Bukowiecki, N., Chen, X., Duplissy, J., Gysel, M., Hutterli, M., Kangasluoma, J., Kontkanen, J., Kürten, A., Manninen, H. E., Münch, S., Peräkylä, O., Petäjä, T., Rondo, L., Williamson, C., Weingartner, E., Curtius, J., Worsnop, D. R., Kulmala, M., Dommen, J. and Baltensperger, U.: New particle formation in the free troposphere: A question of chemistry and timing, Science, 352(6289), 1109–1112, doi:10.1126/science.aad5456, 2016.

EPA: Quality Assurance Handbook for Air Pollution Measurement Systems, Volume IV: Meteorological measurements, 2008.

Hammer, E., Bukowiecki, N., Gysel, M., Jurányi, Z., Hoyle, C. R., Vogt, R., Baltensperger, U. and Weingartner, E.: Investigation of the effective peak supersaturation for liquid-phase clouds at the high-alpine site Jungfraujoch, Switzerland (3580 m a.s.l.), Atmos. Chem. Phys., 14(2), 1123–1139, doi:10.5194/acp-14-1123-2014, 2014.

Herrmann, E., Weingartner, E., Henne, S., Vuilleumier, L., Bukowiecki, N., Steinbacher, M., Conen, F., Collaud Coen, M., Hammer, E., Jurányi, Z., Baltensperger, U. and Gysel, M.: Analysis of long-term aerosol size distribution data from Jungfraujoch with emphasis on free tropospheric conditions, cloud influence, and air mass transport, J. Geophys. Res. Atmos., 120(18), 2015JD023660, doi:10.1002/2015JD023660, 2015.

Hirsikko, A., Laakso, L., Horrak, U., Aalto, P. P., Kerminen, V. and Kulmala, M.: Annual and size dependent variation of growth rates and ion concentrations in boreal forest, Boreal Environ. Res., 10(5), 357, 2005.

Hirsikko, A., Bergman, T., Laakso, L., Dal Maso, M., Riipinen, I., Hõrrak, U. and Kulmala, M.: Identification and classification of the formation of intermediate ions measured in boreal forest, Atmos. Chem. Phys., 7(1), 201–210, doi:10.5194/acp-7-201-2007, 2007.

IPCC: IPCC (AR5):Climate change 2013: The Physical Science Basis, Summary for policymakers. Contribution of Working Group I to the Fifth Assesment report, 2013.

Jurányi, Z., Gysel, M., Weingartner, E., Bukowiecki, N., Kammermann, L. and Baltensperger, U.: A 17 month climatology of the cloud condensation nuclei number concentration at the high alpine site Jungfraujoch, J. Geophys. Res., 116(D10), D10204, doi:10.1029/2010JD015199, 2011.

Kerminen, V.-M., Paramonov, M., Anttila, T., Riipinen, I., Fountoukis, C., Korhonen, H., Asmi, E., Laakso, L., Lihavainen, H., Swietlicki, E., Svenningsson, B., Asmi, A., Pandis, S. N., Kulmala, M. and Petäjä, T.: Cloud condensation nuclei production associated with atmospheric nucleation: a synthesis based on existing literature and new results, Atmos. Chem. Phys., 12(24), 12037–12059, doi:10.5194/acp-12-12037-2012, 2012.

Komppula, M., Lihavainen, H., Kerminen, V.-M., Kulmala, M. and Viisanen, Y.: Measurements of cloud droplet activation of aerosol particles at a clean subarctic background site, J. Geophys. Res. Atmos. (1984–2012), 110(D6), 2005.

Kulmala, M. and Kerminen, V.-M.: On the formation and growth of atmospheric nanoparticles, Atmos. Res., 90(2–4), 132–150, doi:10.1016/j.atmosres.2008.01.005, 2008.

Kulmala, M., Riipinen, I., Sipilä, M., Manninen, H. E., Petäjä, T., Junninen, H., Maso, M. D., Mordas, G., Mirme, A., Vana, M., Hirsikko, A., Laakso, L., Harrison, R. M., Hanson, I., Leung, C., Lehtinen, K. E. J. and Kerminen, V.-M.: Toward Direct Measurement of Atmospheric Nucleation, Science, 318(5847), 89–92, doi:10.1126/science.1144124, 2007.

Laakso, L., Merikanto, J., Vakkari, V., Laakso, H., Kulmala, M., Molefe, M., Kgabi, N., Mabaso, D., Carslaw, K. S., Spracklen, D. V., Lee, L. A., Reddington, C. L. and Kerminen, V.-M.: Boundary layer nucleation as a source of new CCN in savannah environment, Atmos. Chem. Phys., 13(4), 1957–1972, doi:10.5194/acp-13-1957-2013, 2013.

Laaksonen, A., Hamed, A., Joutsensaari, J., Hiltunen, L., Cavalli, F., Junkermann, W., Asmi, A., Fuzzi, S. and Facchini, M. C.: Cloud condensation nucleus production from nucleation events at a highly polluted region, Geophys. Res. Lett., 32(6), 2005.

Lee, L. A., Pringle, K. J., Reddington, C. L., Mann, G. W., Stier, P., Spracklen, D. V., Pierce, J. R. and Carslaw, K. S.: The magnitude and causes of uncertainty in global model simulations of cloud condensation nuclei, Atmos. Chem. Phys., 13(17), 8879–8914, doi:10.5194/acp-13-8879-2013, 2013.

Lihavainen, H., Kerminen, V.-M., Komppula, M., Hatakka, J., Aaltonen, V., Kulmala, M. and Viisanen, Y.: Production of “potential” cloud condensation nuclei associated with atmospheric new-particle formation in northern Finland, J. Geophys. Res. Atmos. (1984–2012), 108(D24), 2003.

Makkonen, R., Asmi, A., Kerminen, V.-M., Boy, M., Arneth, A., Hari, P. and Kulmala, M.: Air pollution control and decreasing new particle formation lead to strong climate warming, Atmos. Chem. Phys., 12(3), 1515–1524, doi:10.5194/acp-12-1515-2012, 2012.

Manninen, H. E., Mirme, S., Mirme, A., Petäjä, T., and Kulmala, M.: How to reliably detect molecular clusters and nucleation mode particles with Neutral cluster and Air Ion Spectrometer (NAIS), Atmos. Meas. Tech., 9, 3577-3605, doi:10.5194/amt-9-3577-2016, 2016.

Merikanto, J., Spracklen, D. V., Mann, G. W., Pickering, S. J. and Carslaw, K. S.: Impact of nucleation on global CCN, Atmos. Chem. Phys., 9(21), 8601–8616, doi:10.5194/acp-9-8601-2009, 2009.

Mirme, S. and Mirme, A.: The mathematical principles and design of the NAIS – a spectrometer for the measurement of cluster ion and nanometer aerosol size distributions, Atmos. Meas. Tech., 6(4), 1061–1071, doi:10.5194/amt-6-1061-2013, 2013.

Mitchell, A. E.: A comparison of short-term dispersion estimates resulting from various atmospheric stability classification methods, Atmos. Environ. (1967), 16(4), 765–773, doi:10.1016/0004-6981(82)90394-8, 1982.

Mitchell, A. E. and Timbre, K. O.: Atmospheric stability class from horizontal wind fluctuation, Proceedings of the LXXII Annual Meeting of the Air Pollution Control Association, 79–29.2, 1979.

Pierce, J. R., Leaitch, W. R., Liggio, J., Westervelt, D. M., Wainwright, C. D., Abbatt, J. P. D., Ahlm, L., Al-Basheer, W., Cziczo, D. J., Hayden, K. L. and others: Nucleation and condensational growth to CCN sizes during a sustained pristine biogenic SOA event in a forested mountain valley, Atmos. Chem. Phys., 12(7), 3147–3163, 2012.

Reddington, C. L., Carslaw, K. S., Spracklen, D. V., Frontoso, M. G., Collins, L., Merikanto, J., Minikin, A., Hamburger, T., Coe, H., Kulmala, M., Aalto, P., Flentje, H., Plass-Dülmer, C., Birmili, W., Wiedensohler, A., Wehner, B., Tuch, T., Sonntag, A., O'Dowd, C. D., Jennings, S. G., Dupuy, R., Baltensperger, U., Weingartner, E., Hansson, H.-C., Tunved, P., Laj, P., Sellegri, K., Boulon, J., Putaud, J.-P., Gruening, C., Swietlicki, E., Roldin, P., Henzing, J. S., Moerman, M., Mihalopoulos, N., Kouvarakis, G., Ždímal, V., Zíková, N., Marinoni, A., Bonasoni, P. and Duchi, R.: Primary versus secondary contributions to particle number concentrations in the European boundary layer, Atmos. Chem. Phys., 11(23), 12007–12036, doi:10.5194/acp-11-12007-2011, 2011.

Roberts, G. C. and Nenes, A.: A continuous-flow streamwise thermal-gradient CCN chamber for atmospheric measurements, Aer. Sci. Technol., 39(3), 206–221, 2005.

Roberts, G. C., Day, D. A., Russell, L. M., Dunlea, E. J., Jimenez, J. L., Tomlinson, J. M., Collins, D. R., Shinozuka, Y. and Clarke, A. D.: Characterization of particle cloud droplet activity and composition in the free troposphere and the boundary layer during INTEX-B, Atmos. Chem. Phys., 10(14), 6627–6644, doi:10.5194/acp-10-6627-2010, 2010.

Rose, C., Sellegri, K., Velarde, F., Moreno, I., Ramonet, M., Weinhold, K., Krejci, R., Andrade, M., Wiedensohler, A. and Laj, P.: Frequent nucleation events at the high altitude station of Chacaltaya (5240 m a.s.l.), Bolivia, Atmos. Environ., 102, 18–29, doi:10.1016/j.atmosenv.2014.11.015, 2015a.

Rose, C., Sellegri, K., Asmi, E., Hervo, M., Freney, E., Colomb, A., Junninen, H., Duplissy, J., Sipilä, M., Kontkanen, J., Lehtipalo, K. and Kulmala, M.: Major contribution of neutral clusters to new particle formation at the interface between the boundary layer and the free troposphere, Atmos. Chem. Phys., 15(6), 3413–3428, doi:10.5194/acp-15-3413-2015, 2015b.

Seaton, A., Godden, D., MacNee, W. and Donaldson, K.: Particulate air pollution and acute health effects, The Lancet, 345(8943), 176–178, doi:10.1016/S0140-6736(95)90173-6, 1995.

Spracklen, D. V., Carslaw, K. S., Kulmala, M., Kerminen, V.-M., Sihto, S.-L., Riipinen, I., Merikanto, J., Mann, G. W., Chipperfield, M. P. and Wiedensohler, A.: Contribution of particle formation to global cloud condensation nuclei concentrations, Geophys. Res. Lett., 35(6), 2008.

Tröstl, J., Herrmann, E., Frege, C., Bianchi, F., Molteni, U., Bukowiecki, N., Hoyle, C. R., Steinbacher, M., Weingartner, E., Dommen, J., Gysel, M. and Baltensperger, U.: Contribution of new particle formation to the total aerosol concentration at the high altitude site Jungfraujoch (3’580 m a.s.l., Switzerland), J. Geophys. Res. Atmos., 2015JD024637, doi:10.1002/2015JD024637, 2016.

Twomey, S.: The influence of pollution on the shortwave albedo of clouds, J. Atmos. Sci., 34(7), 1149–1152, 1977.

Weber, R. O.: Estimators for the Standard Deviation of Horizontal Wind Direction, J. Appl. Meteor., 36(10), 1403–1415, doi:10.1175/1520-0450(1997)036<1403:EFTSDO>2.0.CO;2, 1997.

Wex, H., McFiggans, G., Henning, S. and Stratmann, F.: Influence of the external mixing state of atmospheric aerosol on derived CCN number concentrations, Geophysical Research Letters, 37(10) [online] Available from: http://onlinelibrary.wiley.com/doi/10.1029/2010GL043337/full (Accessed 21 February 2014), 2010.

Wiedensohler, A., Birmili, W., Nowak, A., Sonntag, A., Weinhold, K., Merkel, M., Wehner, B., Tuch, T., Pfeifer, S., Fiebig, M., Fjäraa, A. M., Asmi, E., Sellegri, K., Depuy, R., Venzac, H., Villani, P., Laj, P., Aalto, P., Ogren, J. A., Swietlicki, E., Williams, P., Roldin, P., Quincey, P., Hüglin, C., Fierz-Schmidhauser, R., Gysel, M., Weingartner, E., Riccobono, F., Santos, S., Grüning, C., Faloon, K., Beddows, D., Harrison, R., Monahan, C., Jennings, S. G., O'Dowd, C. D., Marinoni, A., Horn, H.-G., Keck, L., Jiang, J., Scheckman, J., McMurry, P. H., Deng, Z., Zhao, C. S., Moerman, M., Henzing, B., de Leeuw, G., Löschau, G. and Bastian, S.: Mobility particle size spectrometers: harmonization of technical standards and data structure to facilitate high quality long-term observations of atmospheric particle number size distributions, Atmospheric Measurement Techniques, 5(3), 657–685, doi:10.5194/amt-5-657-2012, 2012.

Yamartino, R. J.: A Comparison of Several "Single-Pass" Estimators of the Standard Deviation of Wind Direction, Journal of Climate and Applied Meteorology, 23(9), 1362–1366, doi:10.1175/1520-0450(1984)023<1362:ACOSPE>2.0.CO;2, 1984.

Yli-Juuti, T., Riipinen, I., Aalto, P. P., Nieminen, T., Maenhaut, W., Janssens, I. A., Claeys, M., Salma, I., Ocskay, R. and Hoffer, A.: Characteristics of new particle formation events and cluster ions at K-puszta, Hungary, Boreal Environment Research, 14(4), 683–698, 2009.

Yli-Juuti, T., Nieminen, T., Hirsikko, A., Aalto, P. P., Asmi, E., Hõrrak, U., Manninen, H. E., Patokoski, J., Dal Maso, M., Petäjä, T., Rinne, J., Kulmala, M. and Riipinen, I.: Growth rates of nucleation mode particles in Hyytiälä during 2003−2009: variation with particle size, season, data analysis method and ambient conditions, Atmos. Chem. Phys., 11(24), 12865–12886, doi:10.5194/acp-11-12865-2011, 2011.

Table 1 Estimation of the median seasonal and annual CCN productions during NPF events.

	CCN_{50} (cm^{-3})	CCN_{80} (cm^{-3})	CCN_{100} (cm^{-3})
Dry season	3.96×10^{5}	1.60×10^{5}	9.40×10^{4}
Wet season	8.48×10^{4}	4.98×10^{4}	3.90×10^{4}
Whole year	4.81×10^{5}	2.10×10^{5}	1.33×10^{5}

Table 2 Estimation of the median seasonal and annual CCN increases from NPF, i.e. corrected for the contribution of particles transported to the site.

	CCN_{50} (cm^{-3})	CCN_{80} (cm^{-3})	CCN_{100} (cm^{-3})
Dry season	2.00×10^{5}	7.71×10^{4}	4.92×10^{4}
Wet season	5.39×10^{4}	2.13×10^{4}	1.48×10^{4}
Whole year	2.54×10^{5}	9.84×10^{4}	6.40×10^{4}

Table 3 Description of the scenarios concerning the location of the station in the troposphere (boundary layer (BL), interface layer (IL) and free troposphere (FT)) during the first steps of the NPF process, i.e. from the appearance of the newly formed clusters (< 3nm) to the time at which the concentration of 3-7 nm particles was maximum. The total number of occurrence is provided for each scenario in the second column. Since multiple events are frequently observed at Chacaltaya, a more detailed classification including the event position is specified in the last two columns.

Scenario	Description	Total number of occurrence	Single and first position events	Second and following events
S1	First steps of NPF occur in BL	217	100	117
S2		77	68	9
S2.1	First steps of NPF occur in FT	12	7	5
S2.2	Nucleation occurs in FT and initial particle growth is observed in changing conditions, from FT to IL/BL	65	61	4

Table 4. CCN production as a function of the location of the station (BL or FT) at the onset of the NPF process.

Threshold CCN size	CCN increase for events started in the BL (cm^{-3})			CCN increase for events started in the FT (cm^{-3})		
	25th perc.	Median	75th perc.	25th perc.	Median	75th perc.
50 nm	2556	5072	10110	3070	5137	9378
80 nm	1155	2416	3919	1483	2138	5173
100 nm	820	1518	2338	960	1447	3568

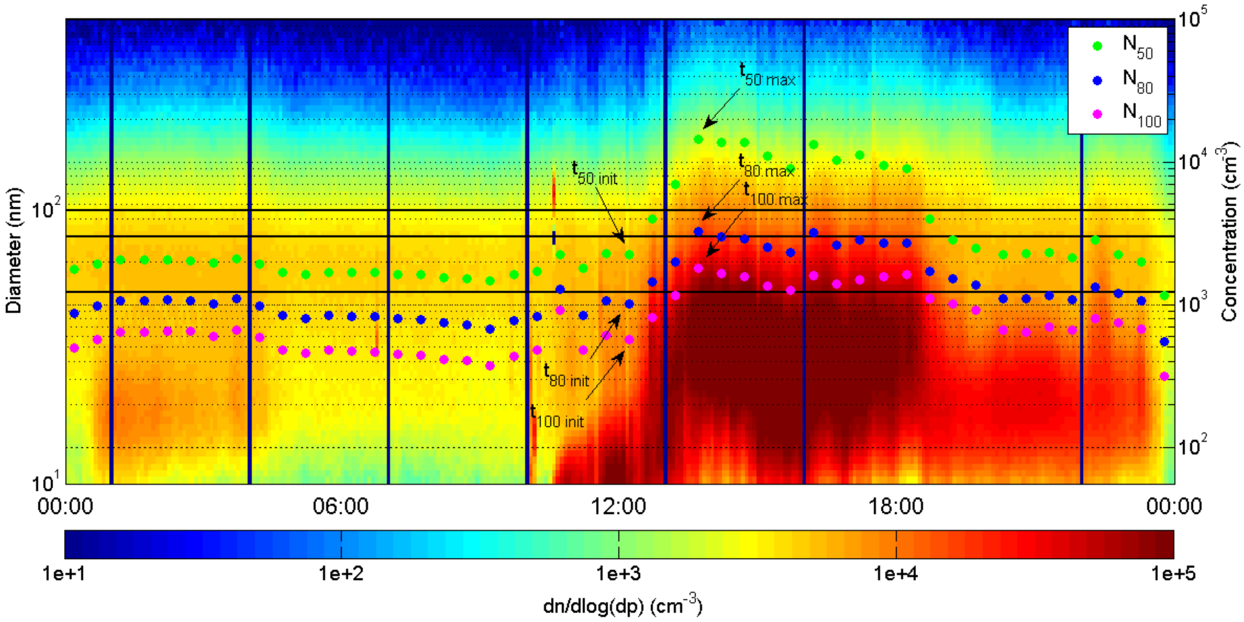

Fig. 1. Determination of the CCN concentration increase for the 3 threshold diameters (50, 80 and 100 nm) from the particle size distributions measured by SMPS. t_{init} and t_{max} denote, for each diameter, the times from which concentration increases are calculated. July 24th 2012.

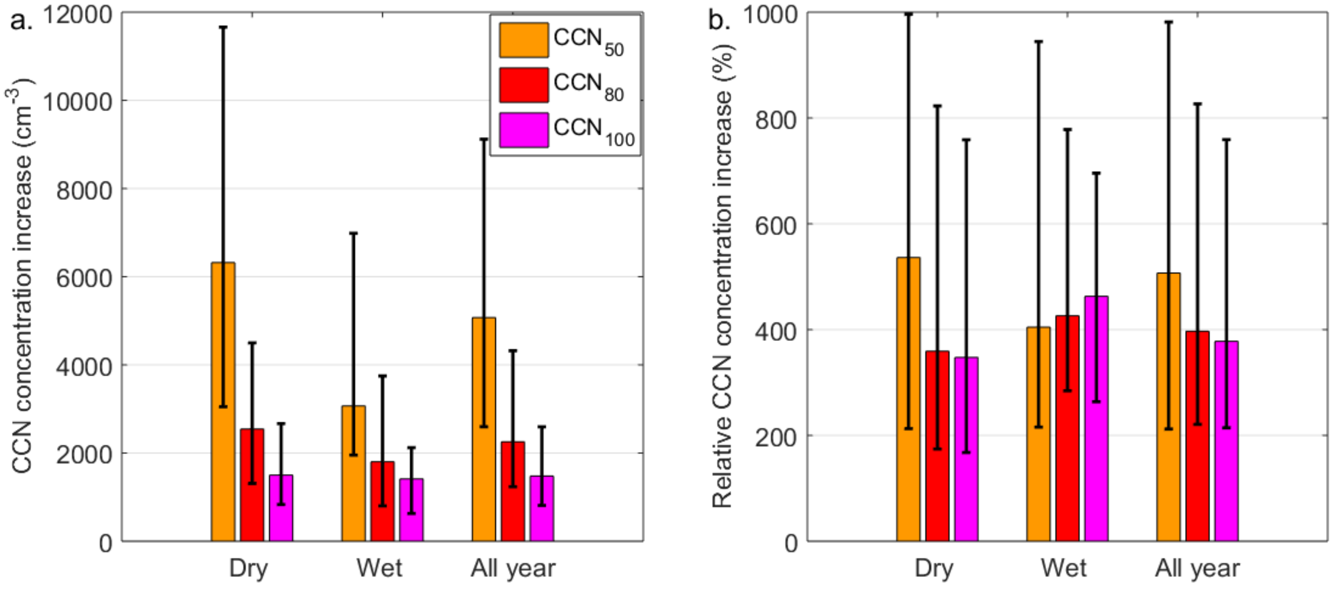

Fig. 2. Median a. absolute and b. relative CCN productions observed during type I events for the different activation diameters and seasons (wet and dry). Lower and upper limits of the error bars stand for the 1st and 3rd quartile, respectively.

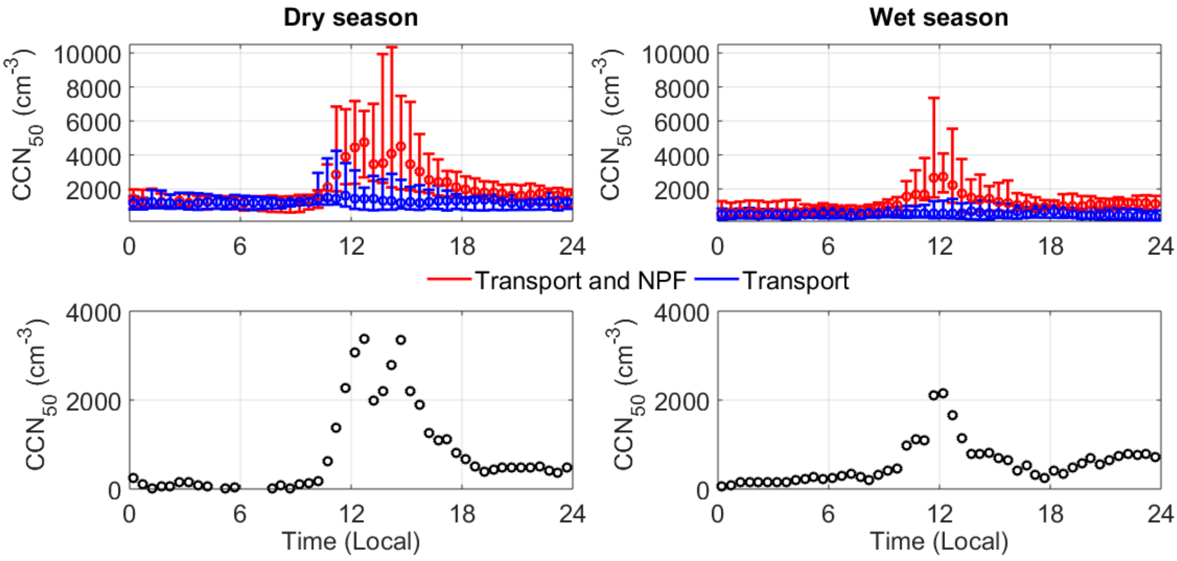

Fig. 3. Median diurnal variation of CCN_{50} on event (upper panel, "Transport and NPF") and non-event days (upper panel, "Transport"). CCN_{50} attributed to NPF (lower panel) is calculated as the difference of the concentrations recorded on event and non-event days. Lower and upper limits of the error bars stand for the 1st and 3rd quartile, respectively.

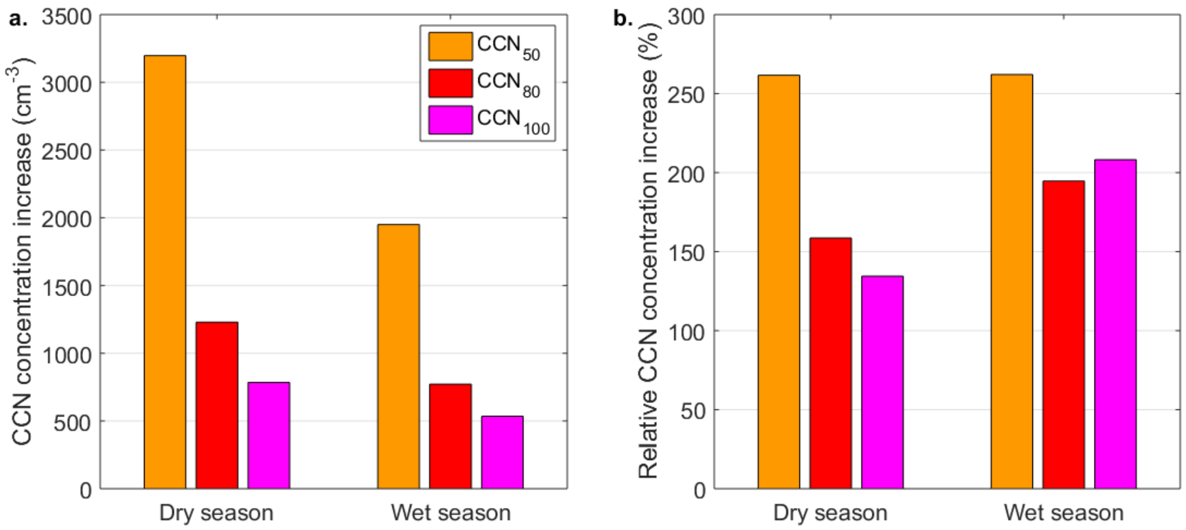

Fig. 4. Median a. absolute and b. relative CCN productions from NPF, i.e. corrected for the transport of CCN-size particles to the site, for the different activation diameters and seasons (wet and dry).

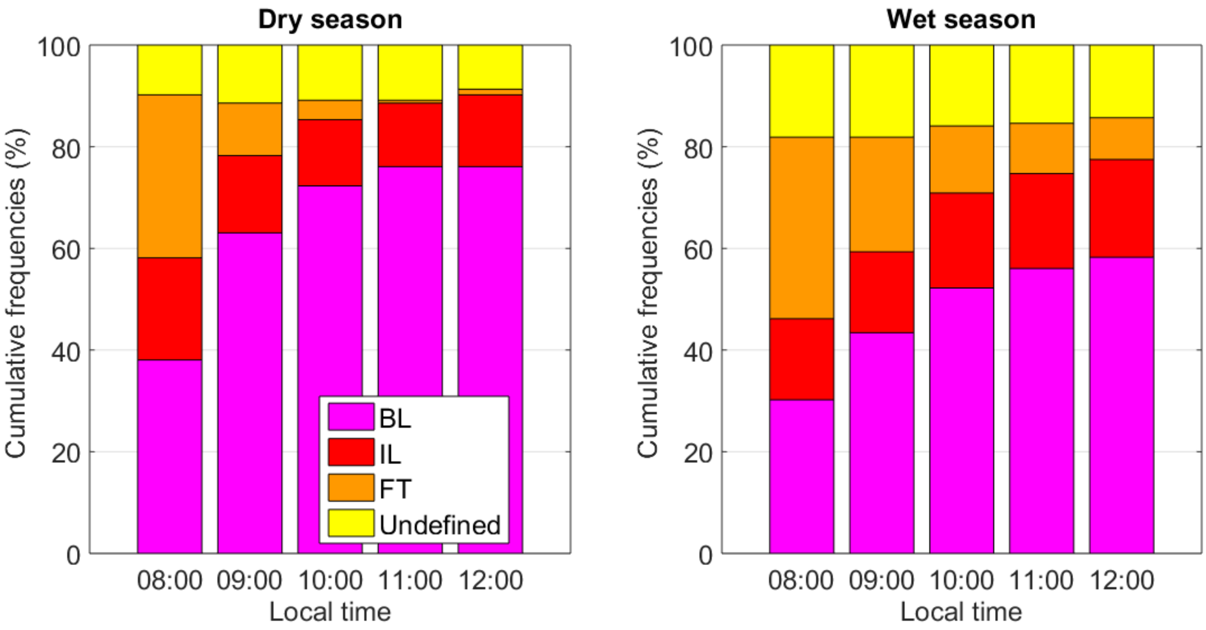

Fig. 5. Statistics on the location of the station in the tropospheric layers (boundary layer (BL), interface layer (IL) and free troposphere (FT)) between 8:00 and 12:00 (Local), separately for the dry and wet seasons.

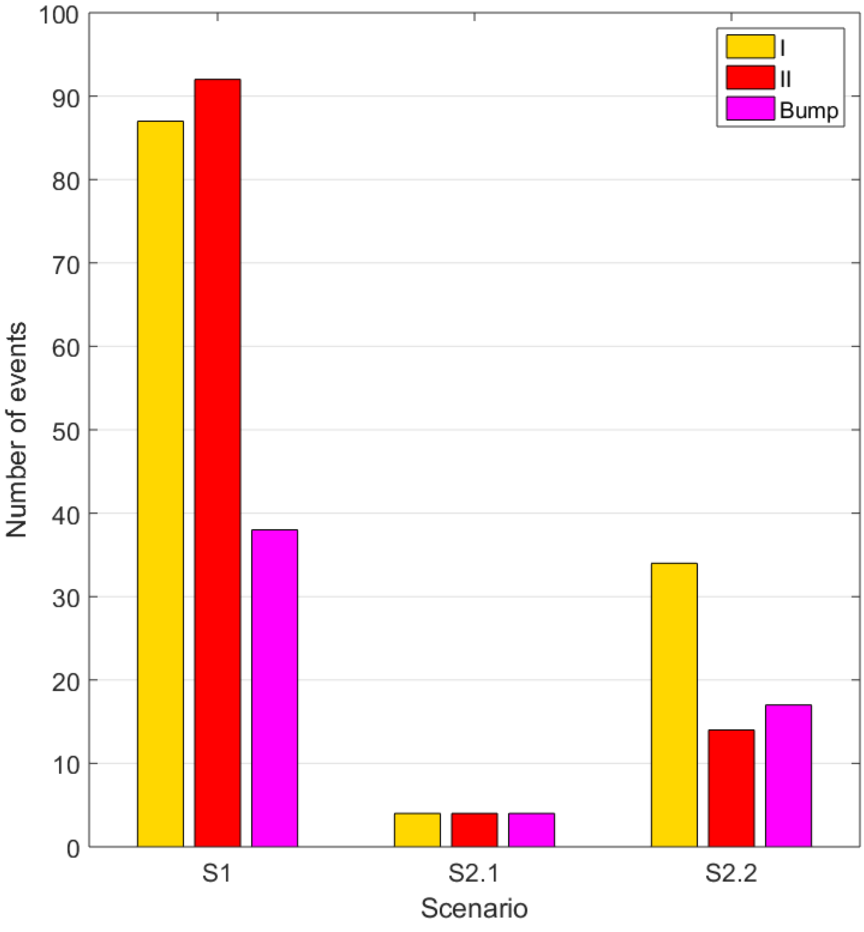

Fig. 6. Statistics on the event type (I, II or bump) as a function of the scenario describing the location of the station in the tropospheric layers (see Table 3).

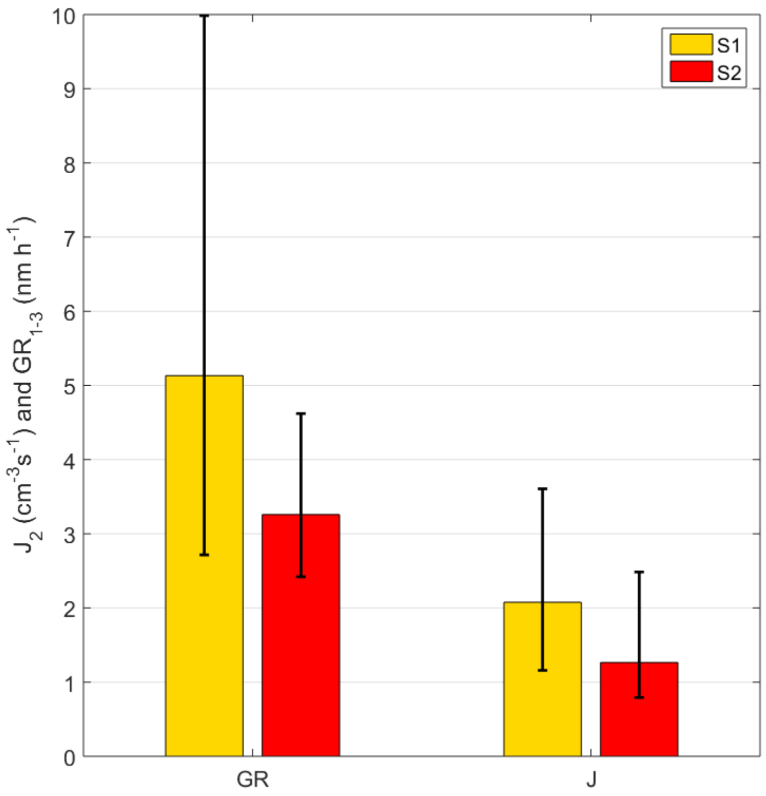

Fig. 7. Median formation rate of 2 nm particles (J_2) and growth rate in the range 1-3 nm ($GR_{1\text{-}3}$) reported separately for type I events initiated in the BL (scenario S1) and in the FT (scenario S2). Lower and upper limits of the error bars stand for the 1st and 3rd quartile, respectively.